LA-UR-02-4089
Approved for public release;
distribution is unlimited.

Title: **Adaptive Time Integration for Hyperbolic Conservation Equations**

Author(s): William J. Rider, Len G. Margolin, and James R. Kamm

Submitted to:

http://lib-www.lanl.gov/cgi-bin/getfile?0105381.pdf

Adaptive Time Integration for Hyperbolic Conservation Equations

William J. Rider, Len G. Margolin, and James R. Kamm

Los Alamos National Laboratory, Los Alamos, NM 87545, USA
wjr@lanl.gov,len@lanl.gov,kammj@lanl.gov

Summary. We introduce a fundamentally new time integration method for hyperbolic conservation laws based on self-adaptivity of the temporal method itself. The adaptivity is based upon the smoothness of the solution measured locally in time. Our approach can be contrasted with the usual global selection of a time integration methods and error-based time step selection methodology. A challenge to this approach is maintaining the adaptivity and the conservation form. These methods are challenged with several standard problems as well as high-resolution experimental data of shock-driven mixing (Richtmyer-Meshkov).

1 Introduction

There have been two major approaches to improving time accuracy in numerical methods for hyperbolic conservation laws: the Lax-Wendroff [3] approach, and the method-of-lines [8]. Both of these are "linear" schemes in the sense that the same time differencing method is applied everywhere in the computational domain, usually for each time-step[1]. We distinguish these from "nonlinear" schemes, implying that the differencing depends on the local flow variables. In this sense, any nonlinear character in standard approaches to time differencing arises from the spatial differencing.

Nonlinear differencing in space has become a standard methodology during the last twenty years, and is generally considered to be essential in effectively solving a broad range of applications. In this research, we explore the utility of nonlinear differencing in time, distinct from that used in space. We describe a methodology that allows the time and space differencing to adapt independently, and locally rather than globally. Finally, we examine the performance of this approach and show a situation where this method appears to yield greatly improved results.

We note that robust software for ordinary differential equations often adjusts the order of the integration scheme based on the local characteristics of the solution [1]. However, in that case the selected order of integration is typically applied to the entire system of ODEs. Extending this approach to a

[1] Runge-Kutta methods are nonlinear in terms of Δt, that is their effective errors are nonlinear in terms of the step size, but linear in the sense that the method is not adapted to the nature of the local solution.

method-of-lines for hyperbolic conservation laws leads to a differencing that is global in space and time with temporal adaptivity, i.e., the same differencing is applied globally in space during a time-step, but varies from one time-step to the next. For example, the order is typically lowered when the estimates of the ordered expansion coefficients do not form a convergent sequence. On the other hand, if the coefficients indicate that the solution is smooth, the order might be increased. Such an approach would forfeit the advantages of modern shock capturing methods, where the order of integration is also spatially dependent upon the local (spatial) character of the solution. In particular, a shock wave is a local phenomenon whose presence should not necessitate the degradation of accuracy in smoother areas of the flow.

Lax-Wendroff techniques implicitly invoke the assumption of space-time similarity. It is assumed that the spatial truncation error will dominate the higher order temporal errors, guaranteeing a dissipative approximation and hence computational stability. While this situation may hold in many circumstances where the phenomena are (approximately) self-similar, it is not general. In particular, near a critical point, where the characteristic speed is nearly zero, the dissipation may vanish, thereby allowing higher-order terms to dominate. In our time adaptive methods, we define new "limiters" that depend on the time derivatives in a manner similar to the manner in which spatial limiters depend on spatial derivatives. In particular, we employ a nonlinear combination of time-differencing methods in the same manner that "upwind" and "downwind" differences are used to achieve a desired property such as monotonicity or positivity preservation[2].

Our recent experience has shown that some difficulties may arise from other issues besides the breakdown of space-time similarity. Numerical algorithms can be viewed as dynamical systems [9]. One must be careful, therefore when implementing a time-differencing scheme, not to introduce spurious fixed points, which would be problematic for a wide variety of applications, including both steady and dynamic problems. Error control, upon which we base our adaptive time algorithms, has been shown to be an effective manner of combating spurious fixed points in solutions.

In the following section, we will describe a basic design of adaptive time integration methods starting with the blending of a linear multistep method with a forward-in-time integrator. Next, we show some results obtained with this method in Section 3. Finally, we will extend this approach introducing a temporal integrator that blends Runge-Kutta methods with weighted ENO ideas. This is described in Section 4.

[2] One must take care when reducing the order of the temporal differencing; when coupled with high-order spatial differencing, the potential for oscillatory behavior arises. Where this is an issue, we drop the spatial accuracy as necessary to maintain stability.

2 Initial Design

In designing our new methodology, we require that each cell edge allow an independent temporal integrator so that the resulting methods remain in conservation form. Thus, in one dimension we choose

$$u_j^{n+1} = u_j^n - \lambda \left[f(u)_{j+\frac{1}{2}} - f(u)_{j-\frac{1}{2}} \right], \tag{1}$$

where $f(u)_{j+\frac{1}{2}}$ has an order of time accuracy that is independent of any other edges. Here, u is the discretized dependent variable and f is the associated flux. Subscripts indicate the cell index and superscripts indicate discretized time level. In general, our scheme will depend on the temporal behavior in the zones that determine the flux; e.g., in the simplest case, the limiter will be constructed from u_j and u_{j+1} and its temporal derivatives. Although the spatial limiters will be evaluated at time n, as in the Lax-Wendroff or Runge-Kutta type approaches, we will now need to save previous fluxes or time-derivatives in an Adams-Bashforth fashion.

We have constructed our method in a simple form where temporal differences are tested, through a limiter, in the same manner as spatial differences are used for a Lax-Wendroff-style scheme. The temporal limiter is defined as

$$\widetilde{u_t} = \text{minmod}\left[(u_t)^n, 2(u_t)^{n-1} \right], \text{ or } = \text{minmod}\left[2(u_t)^n, (u_t)^{n-1} \right], \tag{2}$$

where in the most straightforward implementation, $(u_t)^{n-1} = \left(u^n - u^{n-1}\right)/\Delta t$ and $(u_t)^n = -\left[(f(u))_x\right]^n$, as in the Lax-Wendroff approach to time differencing. This is a straightforward form, resulting from using the backwards and forward time derivatives in place of spatial differences in a standard minmod limiter. We note that the extra time differences could be used to raise the temporal accuracy to third order

$$\widetilde{u_t} = \text{minmod}\left[\frac{5}{3}(u_t)^n - \frac{2}{3}(u_t)^{n-1}, 2(u_t)^n, 2(u_t)^{n-1} \right]. \tag{3}$$

There are two distinct outputs resulting from this approach: the actual update of the solution from the previous time step, and the identification of the presence of a critical point (i.e., a sign change in the time derivative). We will examine two cases, using the model equation,

$$\frac{\partial u}{\partial t} + u\frac{\partial u}{\partial x} = g(x,t), \tag{4}$$

i.e., inviscid Burgers' equation with a source term. The first case is a quasi-steady condition, where $\frac{\partial u}{\partial t} \approx 0$ so that $u\frac{\partial u}{\partial x} \approx g(x,t)$. This balance must be maintained for the computations to be well-behaved [5] and achieve the proper steady state. The second, perhaps more interesting case is where $u\frac{\partial u}{\partial x} \approx 0$, implying the balance $\frac{\partial u}{\partial t} \approx g(x,t)$. This indicates the presence

of a stagnation point. Here, the balance between the source term and time derivative must be preserved by the numerical method. The proper evolution of the flow through dynamic critical points is crucial to the overall accuracy of the solution.

3 Tests of The Initial Method

Our initial example is a scalar wave equation where one expects self-similarity to hold. We require from the outset that our methods should perform well in this important cases. The results are shown in Figure 1. In this case the flow is completely self-similar and the new method does not adversely effect the results. In other words, the time-limiter does not turn on except for where the spatial limiting has been activated. We also will examine this method's performance on Burgers' equation.

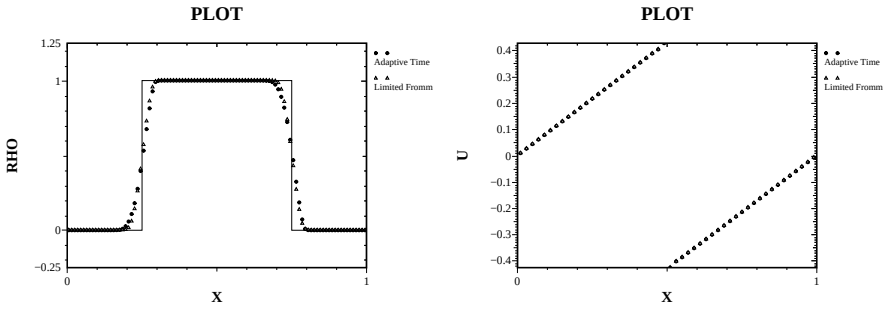

Fig. 1. These two figures basically demonstrate that when self-similarity should hold that the time-limiter does not undermine the method's performance.

For the Euler equations we will start in one dimension. Considering Sod's shock tube, we again see that our new method does not adversely influence the results. This is displayed for the density and velocity fields in Figure 2. Positive aspects of the new method are slightly reduced post shock oscillations and better resolution of the head of the rarefaction. In general, our new approach does not lower the resolution of solutions where self-similarity holds.

Although we expect that multidimensional examples of Euler or Navier-Stokes flows may exhibit more complex behavior than the examples above, we believe it is a necessary prerequisite for our schemes to perform well in these more idealized situations. We conclude by presenting a case where our approach provides a significant improvement for a nontrivial problem. The experiment [7] is a complex example of the evolution of a multidimensional fluid instability. Our attempts to analyze this experiment has provided both

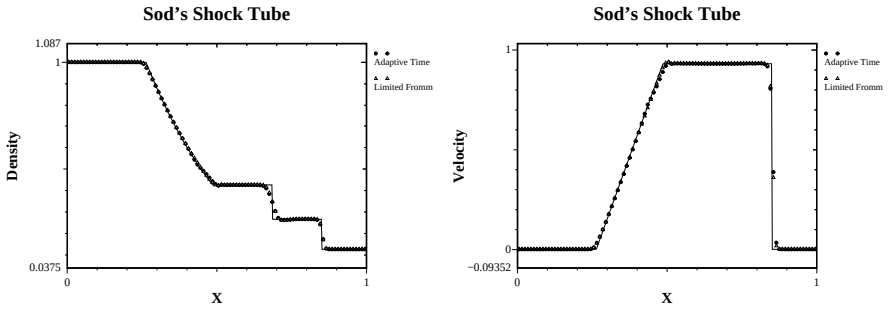

Fig. 2. Results for Sod's shock tube are shown for a limited Fromm's scheme and a spatially limited Fromm's scheme with a time-limiter. The exact solution is given by the solid line.

the initial impetus for our research as well as a framework to judge its utility. We have found that standard high resolution methods such as MUSCL, WENO, DG, TVD, etc., all produce solutions that are not consistent with the *statistical* behavior of the experimental data (as quantified by the fractal dimension, the wavelet spectra and the correlation-based measures of the density field). Of greater concern (and interest), we have found that a first-order Godunov method produces results more consistent with the observed statistical behavior. Further analysis of the simulations has localized the discrepancy to the behavior of the acoustic waves. We have found–and will document–that our adaptive time approach, as discussed above, leads to greatly improved results, in terms of their qualitative and quantitative agreement with the experimental data.

As shown in Figures 3 and 4, the method produces results that are dramatically different than the standard method. This is confirmed by the statistical analysis of these results. The adaptive time method arguably produces the best match to the experimental data both quantitatively and qualitatively as determined by statistical analysis.

4 Extending the Initial Method: Weighted Adaptive Runge-Kutta (WARK)

Buoyed by our initial success, we can extend our method using ideas borrowed from weighted ENO (WENO) methods [4, 2]. Rather than choose weights for a set of spatial stencils, we will choose weights for a series of temporal stencils. The design of the method will follow the general details of a WENO method. The key to this method is the definition of the weights used in the scheme. If the time behavior of the flow is smooth the method will reproduce the high-order result. We name our methods weighted adaptive Runge-Kutta methods (WARK).

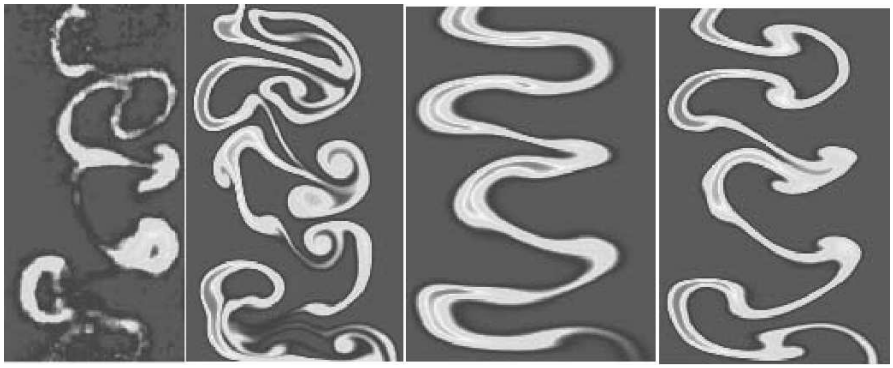

Fig. 3. A montage of images from the gas curtain configuration showing the experimental data at 400 μs, and three simulations initialized from the experimental measurements. From left to right are the experimental images, a standard high-resolution Godunov method, a first-order Godunov method and a high-resolution Godunov method with time limiting. The visual differences in the simulations are striking.

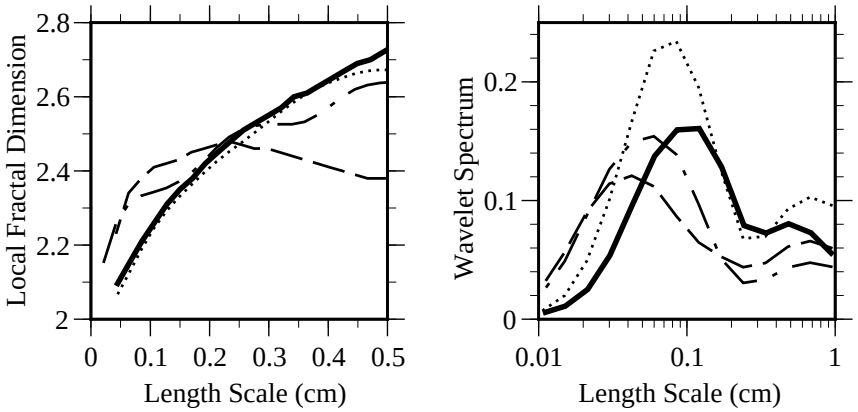

Fig. 4. The statistical analysis of the images shown in Figure 3. The analysis uses fractals and wavelets to measure the properties of the images. The time-limited method is arguably the best match with the experimental statistics. The solid line shows the experimental data, the long dashed line is the standard high-resolution method, the dotted line is the first-order Godunov, and the dot-dashed line is the adaptive time integration.

The steps of this method are identical to other Runge-Kutta methods until the final step of the method where the values are updated to the new time step. For example consider a second-order method (Heun's method) for advancing $u_t = \Psi(u)$:

1. Starting with initial data, $u^0 = u^n$,
2. advance using forward Euler, $u^1 = u^0 + \Delta t \Psi\left(u^0\right)$,
3. also advance the solution for a half time-step (for improved Euler), $u^2 = u^0 + \frac{1}{2}\Delta t \Psi\left(u^0\right)$.
4. before advancing to the new time value of u determine the nonlinear weights, $u^{n+1} = u^n + \Delta t \left\{\frac{1}{2}\omega^0 \left[\Psi\left(u^0\right) + \Psi\left(u^1\right)\right] + \omega^1 \Psi\left(u^2\right)\right\}$.

Note that we have chosen a weighted average of two separate means of advancing the solution at second-order accuracy. The key to this method is defining the weights, ω^k, where $\omega^0 + \omega^1 = 1$. As we will see the general form for the method is

$$u^{n+1} = u^n + \sum_k \omega^k S\left[\Psi\left(u^k\right)\right], \tag{5}$$

where $S(\Psi)$ is a stencil that advances the data with a certain accuracy and $\sum_k \omega_k = 1$ is a constraint. The key is the definition of the nonlinear weights and the self-adaptivity coming from the smoothness indicators, IS^k. In this case both weights have the same linear value of $\bar{\omega} = \left(\frac{1}{2}, \frac{1}{2}\right)$, and we use the time derivative associated with each as IS, thus

$$\hat{\omega}^k = \frac{1}{\left(IS^k + \epsilon\right)^2},$$

where $IS^k = \Psi\left(u^k\right)^2$ and $\epsilon = \times 10^{-6}$. Finally, the weights are normalized using $\omega^k = \hat{\omega}^k / \sum_m \hat{\omega}^m$.

The only remaining issue to rectify is how to define these weights on the fluxes rather than the function evaluations. This is required because we must maintain a conservative discretization in space. We will explore the option where one is to average the two time derivatives in the zones adjacent to a flux,

$$IS^k_{j+\frac{1}{2}} = S\left[\Psi\left(u^k_j\right)\right]^2 + S\left[\Psi\left(u^k_{j+1}\right)\right]^2.$$

A variety of other methods can easily be converted into this general format and made adaptive. For example the popular third-order TVD Runge-Kutta integrator and the classical fourth-order Runge-Kutta methods have been experimented with. For the third-order TVD the only major change necessary is the final step which is modified to read,

$$u^{n+1} = u^n + \Delta t \sum_0^1 \omega^k \Psi\left(u^k\right),$$

with linear weights, $\bar{\omega} = \left(\frac{1}{3}, \frac{2}{3}\right)$. We start with the usual sequence of operations,

$$u^1 = u^0 + \Delta t \Psi\left(u^0\right); u^2 = \frac{3}{4}u^0 + \frac{1}{4}u^1 + \Delta t \Psi\left(u^1\right).$$

The linear stencils are two second-order methods $S\left[\Psi\left(u\right)\right]^1 = \frac{1}{2}\left[\Psi\left(u^0\right) + \Psi\left(u^1\right)\right]$, and $S\left[\Psi\left(u\right)\right]^2 = \Psi\left(u^2\right)$.

Using modified equation analysis, we can see the differences in the properties of the two second-order methods [6]. Applying this approach to examine the time-differencing errors for $\Psi\left(u\right) = -f\left(u\right)_x$ we find the following, for $S\left[\Psi\left(u\right)\right]^1$ the error is

$$\left(\Delta t f'\right)^2 \left(\frac{1}{4}f''\left(u_x\right)^2 + \frac{1}{6}f' u_{xx}\right)_x,$$

where $f' = \partial f\left(u\right)/\partial u$, and $f'' = \partial^2 f\left(u\right)/\partial u^2$ and for $S\left[\Psi\left(u\right)\right]^2$,

$$\left(\Delta t f'\right)^2 \left(\frac{1}{8}f''\left(u_x\right)^2 + \frac{1}{12}f' u_{xx}\right)_x.$$

Both the dissipative and dispersive errors are opposite in sign (required to cancel to achieve third-order), the schemes can successfully adapt to the flow. In particular, the terms proportional to $f''\left(u_x\right)^2$ are (anti)dissipative depending upon the sign of u_x. With this behavior the scheme can adapt locally so that appropriate dissipation can be applied via the time integration scheme.

A classical fourth-order Runge-Kutta can be made adaptive as well. Runge-Kutta methods have been experimented with. For the third-order TVD the only major change necessary is the final step which is modified to read,

$$u^{n+1} = u^n + \Delta t \sum_0^2 \omega^k \Psi\left(u^k\right),$$

with linear weights, $\bar{\omega} = \left(\frac{1}{3}, \frac{1}{3}, \frac{1}{3}\right)$. We start with the usual sequence of operations,

$$u^1 = u^0 + \frac{1}{2}\Delta t \Psi\left(u^0\right); u^2 = u^0 + \frac{1}{2}\Delta t \Psi\left(u^1\right); u^3 = u^0 + \Delta t \Psi\left(u^2\right).$$

The linear stencils are two second-order methods $S\left[\Psi\left(u\right)\right]^0 = \frac{1}{2}\left[\Psi\left(u^0\right) + \Psi\left(u^3\right)\right]$, $S\left[\Psi\left(u\right)\right]^1 = \Psi\left(u^1\right)$, and $S\left[\Psi\left(u\right)\right]^2 = \Psi\left(u^2\right)$.

Now we will test these methods on a simple, self-similar case. As shown in Figure 5 the method produce small changes over the standard methods in this case.

We find that for a self similar flow, the solutions are not perturbed by the adaptivity in time.

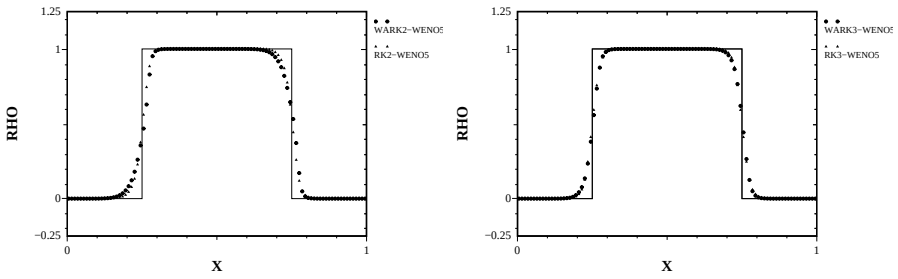

Fig. 5. The basic performance of the WARK method for a scalar wave equation and 5th order WENO differencing in space as compared with the "linear" time differencing that forms the basis of the scheme used.

5 Summary

In summary, we have only begun to explore the possible formulations of time adaptivity. We believe that our preliminary results illustrate the power and flexibility of the approach, as well as its effectiveness. In particular, the ability to deal with problems that do not exhibit hyperbolic self-similarity should provide a new approach to attacking this difficult and important class of problems.

Acknowledgments

Also available as Los Alamos National Laboratory Report, LA–UR–02–4089. This work performed under the auspices of the U.S. Department of Energy by Los Alamos National Laboratory under Contract W-7405-ENG-36. Direct support for this research was provided by the Laboratory Directed Research and Development (LDRD) program.

References

1. U. M. Ascher and L. R. Petzold, *Computer Methods for Ordinary Differential Equations and Differential-Algebraic Equations*, SIAM, Philadelphia, PA, 1996.
2. G.-S. Jiang and C.-W. Shu, Efficient of Weighted ENO Methods, *J. Comp. Phys.*, **126**, 202-228, 1996.
3. P. D. Lax and B. Wendroff, Systems of Conservation Laws, *Communications in Pure and Applied Mathematics*, **13**:217–237, 1960.
4. X.-D. Liu, S. Osher and T. Chan, Weighted Essentially Non-Oscillatory Schemes, *J.Comp. Phys.*, **115**, 200–212, 1994.
5. L. G. Margolin and D. A. Jones, An Approximate Inertial Manifold for Computing Burgers' Equation, *Physica D*, **60**:175–184, 1992

6. W. J. Rider, L. G. Margolin and J. R. Kamm, Techniques for Analysis of Nonlinear Approximations to Nonlinear Equations, submitted for review, Los Alamos National Laboratory Reportm LA–UR–02–3215, 2002.
7. P. M. Rightley, P. Vorobieff, R. Martin & R. F. Benjamin, Experimental-observations of the mixing transition in a shock-accelerated gas curtain, *Phys. Fluids*, **11**:186–200, 1999.
8. C.-W. Shu,Total-Variation-Diminishing Time Discretizations, *SIAM J. Sci. Comp.*, **9**:1073–1084, 1988.
9. H. C. Yee, N. D. Sandham and M. J. Djomehri, On Spurious Behavior in CFD Simulations, *Int. J. Num. Meth. Fluids*, **30**: 675-711, 1999.